Communication in Photoscience(2015), vol. 4, no. 1, pp. 25-28
http://dx.doi.org/10.5857/RCP.2015.4.1.25 **ISSN 2288-4564(Online)**

Communications

Time-Resolved Photoexcitation Dynamics of Electrical Conductivity of Magnetic Organic Superconductor λ-$(BETS)_2Fe_{0.45}Ga_{0.55}Cl_4$

Farzana Sabeth,[a)] Md. Serajul Islam,[b)] Tadashi Endo, Nobuhiro Ohta*

Research Institute for Electronic Science (RIES), Hokkaido University, Sapporo 001-0020, Japan.

ABSTRACT: The time-resolved photoexcitation dynamics of electrical conductivity of the magnetic organic superconductor λ-$(BETS)_2Fe_{0.45}Ga_{0.55}Cl_4$ has been studied with a nanosecond visible laser pulse at its three different phases, i. e., metallic phase, superconducting phase and insulating phase. A transient increase of the resistance is induced by photoirradiation at all the temperatures measured for all three phases, but the decay profile shows a significant temperature dependence. The relaxation rate in the metallic and insulating phase are different from each other, and the decay time is relatively faster and almost constant in the metallic phase. However, a prolongation of the relaxation time is observed at temperature just around the narrow superconducting phase. Nonbolometric (nonthermal) origin of the observed photoresponse of the electrical conductivity is confirmed in the superconducting phase.

INTRODUCTION

Tuning electrical conductivity by employing external perturbations such as photoirradiation, electric field and/or magnetic field to achieve desired functionalities of molecular conductors is a fascinating topic in material science for the development of innovative optoelectronic materials.[1-4] One of the big challenges is to induce superconductivity using external stimuli. The organic charge transfer complexes appeal to be one of the most promising candidate, as the electron gas of these compounds displays a very rich spectrum of instabilities due to the low dimensionality and strong electron correlation. These instabilities may be induced by different parameters and lead to the unconventional properties like characteristic phase transitions among a variety of phases including a superconducting state, charge ordering, metal-insulator transition, magnetic ordering, and often a competition between different phases. Light induced phase-transition phenomena of molecular conductors have been extensively studied and reported by several research groups: for example, a light-induced charge transfer in a donor–acceptor stacked molecule,[5,6] a photoinduced phase transition from a charge-ordered insulating phase to a metallic phase in the organic conductor α-[bis(ethylenedithio)tetrathiafulvalene]$_2I_3$ [α-(BEDT-TTF)$_2I_3$] by using femtosecond pump probe spectroscopy and time-resolved photoresponse measurements of electrical conductivity.[7-11] Recently the insulator–metal transitions induced by electric field and photoirradiation in organic Mott insulator deuterated κ-$(BEDTTTF)_2Cu[N(CN)_2]Br$ has been reported by our group.[12] Moreover, photoexcitation dynamics of organic superconductors β-$(BEDT\text{-}TTF)_2I_3$ together with its deuterated analog, and hydrogenated compound of κ-$(BEDT\text{-}TTF)_2Cu[N(CN)_2]Br$ was also studied to elucidate the potential of the emergence of photoinduced superconductivity.[13,14] However, the possibility of the photoinduced superconductivity in organic conductors is still enigmatic. Understanding of the photoresponse of the conductivity of organic superconductors is crucial to realize the photoinduced superconductivity.

***To whom correspondence should be addressed.**
E-mail: nohta@es.hokudai.ac.jp

Here, we have studied the photoexcitation dynamics of organic superconductor λ-$(BETS)_2Fe_{0.45}Ga_{0.55}Cl_4$, where BETS is bis(ethylenedithio)tetraselenafulvalene. The BETS molecule is a modified form of BEDT-TTF produced by substituting selenium for sulfur in the central tetrathiafulvalene fragment in order to enhance the quasi two-dimensional (2D) electron properties.[15] BETS and tetrahedral monoanions MX^4 (M = Ga, Fe ; X = C1, Br) have produced many highly conductive compounds.[16] For example, λ-$(BETS)_2GaCl_4$ is an organic superconductor[16] whereas the isostructural λ-$(BETS)_2FeCl_4$ undergoes a phase transition from a paramagnetic metal to an anti-ferromagnetic (AF) insulator at zero magnetic field.[17] When the magnitude of the magnetic field is above 17 T, it exhibits a magnetic field induced superconductivity.[18] In fact, the members of BETS family containing Fe ions are of particular interest because strong competition is expected between the antiferromagnetic order of the Fe moments and the superconductivity, and consequently the BETS conductors with mixed anions, e. g., λ-$(BETS)_2Fe_xGa_{1-x}Cl_4$, have been extensively studied over the past ten years. The Fe-rich crystals of λ-$(BETS)_2Fe_xGa_{1-x}Cl_4$ ($x>0.5$) undergo a sharp metal-insulator (MI) phase transition, and the transition temperature T_{MI} decreases with decreasing the value of x. On the contrary, Ga-rich crystals with $x<0.5$ exhibit a superconducting transition.[19] Being at the borderline, λ-$(BETS)_2(Fe_{0.45}Ga_{0.55})Cl_4$ crystal shows phase variety with temperature at ambient pressure. As the temperature decreases, it undergoes a metal-superconductor phase transition at around 4 K, but after showing a very narrow superconducting phase it further undergoes unprecedented superconductor-antiferromagnetic insulator transitions at a lower temperature (below liquid helium temperature). [20, 21]

EXPERIMENTAL SECTION

Single crystals of λ-$(BETS)_2(Fe_{0.45}Ga_{0.55})Cl_4$ were synthesized electrochemically from an ethanol (10%) chlorobenzene solution containing BETS, $[(C_2H_5)_4N]FeCl_4$ and $[(C_2H_5)_4N]GaCl_4$ in exact proportion.[19] A constant current of 0.1μA was applied for 1 month for the anodic deposition of the crystals. Note that BETS synthesized by KNC Laboratories Co., Ltd. was used.

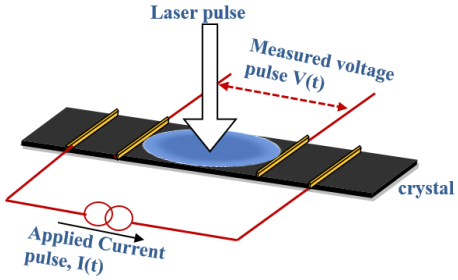

Figure 1. Schematic diagram of the time-resolved measurement of r esistance with laser pulse irradiation.

The needle shaped sample was placed in a cryostat (Optistat CF, Oxford Instruments) which can control temperature in a range of 300 K to 2.5 K. The cooling rate at 80 K was 15 K min^{-1}. Gold wire (10 μm in diameter) and gold paste were used as electrodes. The resistance was measured using the four-probe connection technique. In a steady-state measurement of the temperature dependence of the resistance, the current-reversal method was used with a combination of a current source (Keithley, model 2400) and a nanovolt meter (Keithley, model 2182). As shown in Figure 1, for the time-resolved measurements of the resistance, a constant current of 0.4 mA with a time-width of 40 ms was used, and the attending voltage of the sample was amplified and detected by a digital oscilloscope (104 MXi, LeCroy). The transient change in the resistance was obtained from the voltage waveform divided by the magnitude of the bias current. As a light source, we employed an optical parametric oscillator unit mounting a BBO crystal pumped by a third harmonic of the output of a pulsed Nd:YAG laser (QuantaRay, LAB-150). The pulse width of the output was ~10 ns, and the wavelength of the irradiation light was fixed at 470 nm to excite the absorption band of BETS chromophores. Laser pulse was delivered to the center of the crystal surface between the central electrodes for the voltage measurement (see Figure 1). The direction of the propagation of the laser beam was normal to the needle axis of the crystal and it illuminates an area of diameter 0.4 mm. Though the repetition rate of the laser pulse used was 2 Hz, a single shot of the laser pulse was used to obtain the signal. When the laser pulse was irradiated to the sample, a sharp voltage signal was observed in synchronization with the photoirradiation even without the bias current. For the measurements of the signal due to the photoinduced change of resistance, the photovoltaic component was subtracted from the observed voltage waveform. Moreover, the dark resistance measured by using the pulsed bias current was identical to that obtained by the standard steady-state measurement technique with a smaller current. This observation indicates that the effects of the heating due to the bias current and thermoelectric voltages, which cause an error in the voltage measurements, are negligible in the time resolved experiments.

RESULTS AND DISCUSSION

The magnetic organic superconductor λ-$(BETS)_2Fe_{0.45}Ga_{0.55}Cl_4$ lies in the boundary between the superconducting state and antiferromagnetic insulating state. The temperature dependence of the resistivity of λ-$(BETS)_2Fe_{0.45}Ga_{0.55}Cl_4$ normalized to its room temperature value is represented in Figure 2. The plot indicates successive metal-superconductor and superconductor-insulator transitions as temperature is decreased below liquid helium temperature showing a very narrow superconducting temperature region around 4 K.

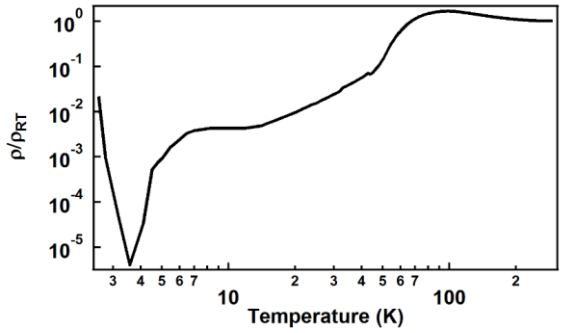

Figure 2. Normalized resistivity of λ-$(BETS)_2Fe_{0.45}Ga_{0.55}Cl_4$ as a function of temperature.

Time profiles of the transient change in resistance (ΔR) with photoirradiation were measured at different temperatures in the metallic, superconducting and insulating region. The results obtained with a laser light intensity of 1.7 μJ/pulse and a bias current of 0.4 mA are demonstrated in Figure 3, where the vertical axis represents the change in resistance and the horizontal axis represents the time elapsed after irradiation of the laser pulse at time t = 0. The signal in the positive direction indicates that the resistance is increased by photoirradiation at all the temperatures, whereas the shape of the time profiles have significant temperature dependence. The observed photoirradiation effects are divided into three phases, depending on the temperature range, that is, metallic phase for T > 4 K, narrow superconducting phase around $T \approx$ 4K, and insulating phase for T < 3.5 K. In the metallic phase (i.e. T > 4 K) the decay profiles have smaller and almost constant peak heights. The time profiles are similar to each other and the resistance has recovered its original value within ~3 ms after photoirradiation with a nanosecond laser pulse. In the narrow superconducting phase (T = 4 K), in contrast, the peak height is maximum and the time profiles are elongated and prolonged up to 40 ms. Again in the antiferromagnetic phase (T <3.5 K) a comparatively sharp recovery of the original resistance is observed. But the decay profiles are different from that of the metallic phase, indicating the coexistence of the superconducting and insulating phases.

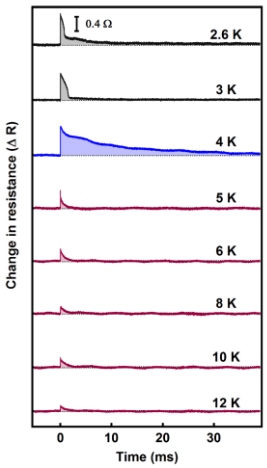

Figure 3. Time profiles of the change in the electrical resistance of λ-$(BETS)_2Fe_{0.45}Ga_{0.55}Cl_4$ in the time range of 0 - 40 ms.

As shown in Figure 3, the time profiles show multiexponential decays, implying the presence of multiple states having a nonequilibrium condition. However, in the present study, the average decay time (τ) was calculated by the following equation considering the decay to be single exponential :

$$(1) \qquad \tau = \frac{\int_0^\infty \Delta R(t)dt}{\Delta R_{peak}}$$

The value of τ can be a measure of the average decay time of the photoinduced change in the resistance. τ as a function of temperature, outlined in Figure 4, describes three different decay times for metallic, superconducting and insulating phases. Although the temperature dependence of decay time is trivial in the metallic phase, a distinct temperature dependence of τ is observed both in the superconducting and in the antiferromagnetic insulator phase (at temperatures below 3.5 K). The relaxation rate shows asymmetry near the superconducting-antiferromagnetic boundary. At temperature ~ 4 K, the decay profile has shown the most prolonged feature.

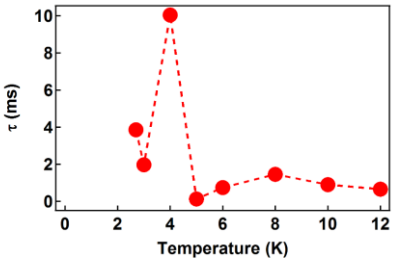

Figure 4. Plots of the average decay time (τ) of the photoinduced change of resistance versus temperature.

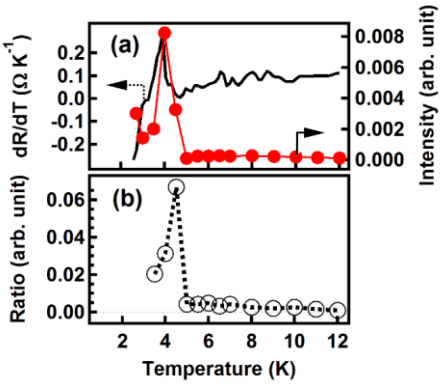

Figure 5. (a) Integrated intensity of the time profile of the resistance change (ΔR) as a function of temperature (closed red circle) and the derivative of the resistance-versus-temperature curve (solid black line) of λ-$(BETS)_2Fe_{0.45}Ga_{0.55}Cl_4$. (b) Ratio of the integrated intensity of ΔR relative to the derivative of $R(T)$ as a function of temperature.

It is noteworthy that the observed photoresponse in the present study is nonbolometric because the temperature rise of the crystal by absorbing the pulsed laser light can not explain such a prominent change in decay profile in the vicinity of superconducting and antiferromagnetic phase. In addition, we have estimated the bolometric response in ΔR: the bolometric photoresponse of the resistance caused by a temperature rise (ΔT) is given by

$$\Delta R_s = \frac{dR(T)}{dT}\Delta T \quad (2)$$

where ΔR_s is the signal intensity and it depends on the derivative of $R(T)$ and ΔT. Figure 5(a) shows the integrated intensity of the time profile of the resistance change (ΔR) as a function of temperature (closed red circle) and a derivative of the resistance-versus-temperature curve (solid black line) of λ-$(BETS)_2Fe_{0.45}Ga_{0.55}Cl_4$. In this analysis, we have used integrated intensity as the signal intensity instead of ΔR_{peak} values, since the integrated intensity is proportional to the laser light intensity. To estimate the difference between integrated intensity and the derivative curves shown in Figure 5(a), the ratio of the integrated intensity relative to the derivative of $R(T)$ is calculated and plotted in Figure 5(b). According to the equation 2, the ratio should be proportional to the temperature rise of the sample if the photoresponse is bolometric. From Figure 5(b) it is clear that the ratio is constant in the metallic phase and increased with the decrease in temperature showing a peak around the superconducting phase. The magnitude of the ratio is much larger than that in the normal metallic phase, especially at 4 K. Such a large change in the ratio, which corresponds to a large change in ΔT (see eq 2), is very much unlikely for a particular temperature. Thus, the origin of the photoresponse in the superconducting phase is clearly nonbolometric and the observed photoresponse arises from the relaxation of photogenerated carriers.[13,14]

In general, the system near the critical point shows a critical slowing down[22] and as mentioned earlier, in photoexcited λ-$(BETS)_2Fe_{0.45}Ga_{0.55}Cl_4$ salt, a slow relaxation dynamics of the resistance has been observed near the superconducting transition temperature. For κ-$(BEDTTTF)_2Cu[N(CN)_2]Br$, which lies in the vicinity of the Mott boundary in the pressure-temperature phase diagram, similar prolongation in the decay time in the superconducting phase was reported by our group.[14] In addition, Iwai et al. have also reported a marked slowing down of the photoexcitation relaxation near superconducting transition temperature using an ultrafast pump-probe reflection spectroscopy.[23] Accordingly, the existence of the slow photoexcited relaxation dynamics might be a special property of the organic superconductors which arises from the complex electronic states.

However, the mechanism of the nonbolometric photoresponse in the superconducting phase of the λ-$(BETS)_2Fe_{0.45}Ga_{0.55}Cl_4$ salt is not clear at present, but photoenhanced flux creep[24] or quasiparticle recombination[25] may be hypothesized as the origin of the observed photoresponse of λ-$(BETS)_2Fe_{0.45}Ga_{0.55}Cl_4$. Further theoretical consideration will be necessary to understand the present results.

CONCLUSION

Time-resolved photoexcitation dynamics of the magnetic organic superconductor λ-$(BETS)_2Fe_{0.45}Ga_{0.55}Cl_4$ has been studied with photoirradiation of the nanosecond laser pulse. The transient increase of the resistance is induced by photoirradiation with a 10 ns laser pulse of wavelength 470 nm. In the metallic phase at temperatures above 4 K, a relatively fast decay profile is observed. At temperatures near Tc, the time profile shows an extremely slow decay. The relaxation rate shows the temperature dependence that was asymmetric with respect to the critical temperature T_c, and asymmetry of the critical slowing down is found. The estimation of the thermal effect using the temperature dependence of the resistance and equation 2 can verify the existence of a nonbolometric photoirradiation effect in the superconducting phase. It is shown that the contribution of the nonbolometric effect to the observed photoresponse becomes larger as the temperature decreases.

KEYWORDS: Electrical conductivity, Photoirradiation effect, Magnetic superconductor, Antiferromagnetic insulator.

Received March 18, 2015; Accepted March 27, 2015

REFERENCES AND NOTES

1. Ohkoshi, S.; Tsunobuchi, Y.; Matsuda, T.; Hashimoto, K.; Namai, A.; Hakoe, F.; Tokoro, H. *Nat. Chem.* **2010,** *2*, 539–545.
2. Ishikawa, T.; Fukazawa, N.; Matsubara, Y.; Nakajima, R.; Onda, K.; Okimoto, Y.; Koshihara, S.; Lorenc, M.; Collet, E.; Tamura, M.; Kato, R. *Phys. Rev. B* **2009,** *80*, 115108.
3. (a) Ueno, K.; Nakamura, S.; Shimotani, H.; Ohtomo, A.; Kimura, N.; Nojima, T.; Aoki, Y.; Iwasa, H.; Kawasaki, M. *Nat. Mater.* **2008,** *7*, 855–858.
   (b) Stoliar, P.; Rozenberg, M.; Janod, E.; Corraze, B.; Tranchant, J.; Cario, L. *Phys. Rev. B* **2014,** *90*, 045146.
4. Iimori, T.; Ohta, N. *J. Phys. Chem. C* **2014,** *118*, 7251–7260.
5. Koshihara, S.; Tokura, Y.; Mitani, T.; Saito, G.; Koda, T. *Phys. Rev. B* **1990,** *42*, 6853–6856.
6. Collet, E.; Lemee-Cailleau, M. H.; Buron-Le Cointe, M.; Cailleau, H.; Wulff, M.; Luty, T.; Koshihara, S. Y.; Meyer, M.; Toupet, L.; Rabiller, P.; Techert, S. *Science*, **2003,** *300*, 612–615.

7. Iwai, S.; Yamamoto, K.; Kashiwazaki, A.; Hiramatsu, F.; Nakaya, H.; Kawakami, Y.; Yakushi, K.; Okamoto, H.; Mori, H.; Nishio, Y. *Phys. Rev. Lett.* **2007,** *98*, 097402.
8. Iimori, T.; Naito, T.; Ohta, N. *J. Am. Chem. Soc.* **2007,** *129*, 3486–3487.
9. Iimori, T.; Naito, T.; Ohta, N. *J. Phys. Chem. C* **2009,** *113*, 4654–4661.
10. Iimori, T.; Ohta, N.; Naito, T. *Appl. Phys. Lett.* **2007,** *90*, 262103.
11. Tajima, N.; Fujisawa, J.; Naka, N.; Ishihara, T.; Kato, R.; Nishio, Y.; Kajita, K. *J. Phys. Soc. Jpn.* **2005,** *74*, 511–514.
12. Sabeth, F.; Iimori, T.; Ohta, N. *J. Am. Chem. Soc.* **2012,** *134*, 6984−6986.
13. Iimori, T.; Sabeth, F.; Naito, T.; Ohta, N. *J. Phys. Chem. C* **2011,** *115*, 23998–24003.
14. Iimori, T.; Naito, T.; Ohta, N. *J. Phys. Chem. C* **2010,** *114*, 9070–9075.
15. Kobayashi, H.; Kobayashi, A.; Cassoux, P. *Chem. Soc. Rev.* **2000,** *29*, 325-333.
16. Kobayashi, A.; Udagawa, T.; Tomita, H.; Naito, T.; Kobayashi, H. *Chem. Lett.* **1993,** *22*, 2179.
17. Tokumoto, M.; Naito, T.; Kobayashi, H.; Kobayashi, A.; Laulhin, V.; Brossard, V. N.; Cassoux, L. *Synth. Met.* **1997,** *86*, 2161.
18. Uji, S.; Shinagawa, H.; Terashima, T.; Yakabe, T.; Terai, Y.; Tokumoto, M.; Kobayashi, A.; Tanaka, H.; Kobayashi, H. *Nature*, **2001,** *410*, 908-910.
19. Kobayashi, H.; Cui, H. B.; Kobayashi, A. *Chem. Rev.* **2004,** *104*, 5265-5288.
20. Kobayashi, H.; Sato, A.; Arai, E.; Akutsu, H.; Kobayashi, K.; Cassoux, P. *J. Am. Chem. Soc.* **1997,** *119*, 12392.
21. (a) Sato, A.; Ojima, E.; Akutsu, H.; Kobayashi, H.; Kobayashi, A.; Cassoux, P. *Chem. Lett.* **1998,** *27*, 673-674.
(b) Sato, A.; Ojima, E.; Akutsu, H.; Nakazawa, Y.; Kobayashi, H.; Tanaka, H.; Kobayashi, A.; Cassoux, P. *Phys. Rev. B* **2000,** *61*, 111.
22. Hohenberg, P. C.; Halperin, B. I. *Rev. Mod. Phys.* **1977**, *49*, 435.
23. Iwai, S.; Yamamoto, K.; Kashiwazaki, A.; Hiramatsu, F.; Nakaya, H.; Kawakami, Y.; Yakushi, K.; Okamoto, H.; Mori, H.; Nishio, Y. *Phys. Rev. Lett.* **2007**, *98*, 097402
24. Zeldof, E.; Amer, N. M.; Koren, G.; Gupta, A. *Phys. Rev. B* **1989**, *39*, 9712–9714.
25. Averitt, R. D.; Taylor, A. J. *J. Phys. Condens. Matter.* **2002**, *14*, 1357–1390.